

Synthesis, Characterization, Surface, and Thermodynamic Studies of Alkyl Tetrachloroferrates: Performance Evaluation of Their Nanostructures as Biocides

Omnia A. A. El-Shamy¹  · Amr O. Habib² · Dalia E. Mohamed¹ · Abdelfattah M. Badawi¹

Received: 5 March 2019 / Revised: 9 July 2019 / Accepted: 19 August 2019
© 2019 AOCS

Abstract Decyl and dodecylamino tetrachloroferrates were synthesized and characterized using Fourier-transform infrared spectroscopy (FTIR), elemental analysis, X-ray diffraction (XRD), nuclear magnetic resonance (¹H-NMR), and atomic absorption spectroscopy (AAS). The surface properties of the cationic surfactants including critical micelle concentration, effectiveness, minimum surface area, and maximum surface excess were determined using surface tension measurements. The effectiveness of surface tension reduction (π_{cmc}) was found to increase as the hydrophobic chain length increases with values of 30 and 34 mN m⁻¹ for C₁₀ and C₁₂, respectively. Moreover, the effect of temperature on micellization was determined over the range of 35–55 °C. Thermodynamic parameters (ΔG° , ΔS° , and ΔH°) were calculated and the results indicate a spontaneous process for both micellization and adsorption. The nanoparticles (NC₁₀ and NC₁₂) of the prepared surfactants were obtained using the ball mill technique. The particle size and morphology of the nanoparticles were determined using transmission electron microscope measurements. The antibacterial study of the nanoparticle surfactants revealed their strong efficiency against fungi and different pathogenic bacteria compared with the original surfactants.

Keywords Quaternary surfactants · Surface activity · Thermodynamic parameters · Nanostructures · Antimicrobial activity

J Surfact Deterg (2019).

Introduction

Surfactants are one of the most important classes of chemicals in colloid and interface science, due to their capability to reduce surface/interfacial tensions and to self-assemble as micelles (Rosen and Kunjappu, 2012). These are amphiphilic compounds comprising hydrophilic head (water-soluble part) and lipophilic tail (oil-soluble part). This dual nature gives them two distinctive characteristics: (i) adsorption; which explains the distinct applications of surfactants (Eastoe and Tabor, 2014; El Feky et al., 2010; Khidr et al., 2015), (ii) self-assembly in solution; which promotes the development of nanoscale structures from biological cells to micelles and microemulsions (Berti and Palazzo, 2014). Therefore, surfactants applied in nanotechnology and related processes such as stabilizers, growth control agents, templates, and modifiers (Garcia et al., 2000).

The number of bacteria with resistance to antibacterial agents has grown over the past decade. Along these lines, it is important to incorporate new compounds that have a microbicide impact (Gaze et al., 2005; Ishikawa et al., 2002; Kourai et al., 2006). Cationic surfactants particularly quaternary ammonium salts are less toxic to human/animals and are utilized in different applications such as biotransformation (Chanawanno et al., 2010). The role of quaternary surfactants as antimicrobial agents can be summarized

Supporting information Additional supporting information may be found online in the Supporting Information section at the end of the article.

✉ Omnia A. A. Elshamy
omniaelshamy@yahoo.com

¹ Egyptian Petroleum Research Institute, 11727, Nasr City, Cairo, Egypt

² Faculty of Engineering, Ain Shams University, Cairo, Egypt

by increasing the permeability of the cell wall of these microorganisms. This causes great harm to the biological balance of the cytoplasm consequently driving to death. Besides, the adsorption of molecules at the cell membrane increases the hydrophobicity of that membrane leading to an increase in its permeability toward the media components. This causes modifications in the biochemical reactions inside the cell cytoplasm (Tezel, 2009).

Nanochemistry is a significant development in nanoscience that bridges the gap between bulk materials and molecular/atomic structures. Nanopowders are solid particles utilized in various applications like ecology, biotechnology, biomedical chemistry, pharmaceutical field, and atomic positioning (Dunkley, 2004; El-Fawal and El-Shamy, 2019; Fraise et al., 2008).

In this work, two quaternary surfactants (decyl amino and dodecyl amino tetrachloroferrate, C_{10} and C_{12} , respectively) are prepared and their chemical structure is reported. The surface activity and thermodynamic parameters at different temperatures were determined. In addition, the nanopowders (NC_{10} and NC_{12}) are obtained from the previously prepared surfactants (parent) using the ball mill technique. The parent surfactants and their nanostructures were evaluated as new potential biocides against pathogenic Gram-positive "*Bacillus pumilus*, *Micrococcus luteus*, and *Sarcina lutea*" and Gram-negative "*Escherichia coli* and *Pseudomonas aeruginosa*" bacteria, Yeast "*Candida albicans*," and some pathogenic fungi "*Penicillium chrysogenum*." The antimicrobial efficiency of the synthesized quaternary surfactants and their nanopowders is included as the inhibition zone diameter "mm mg^{-1} sample" in comparison to Metronidazole for fungus and yeast, and Erythromycin for bacteria as standard drugs.

Experimental Section

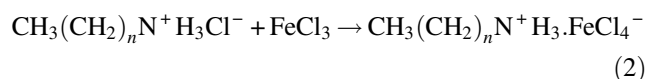
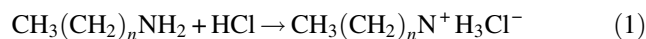
Materials

Dodecyl amine and ferric chloride hexahydrate were obtained from Acros Organics (Geel, Belgium). Decyl amine was obtained from MP Biomedical (Eschwege, Germany). Ethanol and acetone were purchased from ADWIC (Qaliubiya, Egypt). All chemicals were used without further purification.

Synthesis of the Quaternary Surfactants

The two quaternary surfactants were prepared by mixing equal ratios (1:1) of each of decyl amine and dodecyl amine with HCl separately, giving a white precipitate of amine hydrochlorides. Reflux of the obtained amine

hydrochlorides with $FeCl_3$ (1:1) in ethanol for 2 h was carried out at 75 °C. Brown and yellowish brown precipitates for decylamino tetrachloroferrate C_{10} and dodecylamino tetrachloroferrate C_{12} , respectively, were obtained and washed with ethanol several times. The C_{10} and C_{12} reactions are shown in Eqs. (1) and (2):



where $n = 9$ in the case of decylamino tetrachloroferrate and $n = 11$ in the case of dodecylamino tetrachloroferrate.

The nanopowder form of the synthesized surfactants (NC_{10} and NC_{12}) was obtained using a Type PM 400 ball mill (RETSCH Planetary) at 200 rpm for 8 h.

Characterization

Elemental analysis of the prepared surfactants was done using a Vario MACRO Cube (Elementar, Hanau, Germany). A Zeenit 700 P atomic absorption spectrometer (Analytic Jena, Thuringia, Germany) equipped with single-element hollow cathode lamp as a radiation source was used to detect the iron percentage in the prepared surfactants. Fourier-transform infrared (FTIR) (KBr) spectra were recorded using a by ATI Mattson Genesis at an incidence angle of 80° relative to the normal surface and 2 cm^{-1} resolution. 1H -NMR spectra of the compounds under examination were recorded in DMSO at 500 MHz using a Jeol ECA 500 MHz NMR spectrometer. X-ray diffraction (XRD) spectroscopy (PANalytical X'Pert PRO MPD, Netherland) was used to characterize the crystal structure of the prepared surfactants. The XRD instrument was equipped with a Cu anode ($\lambda = 0.154,06$ nm) at a rate of 40 kV with a scan step time of 0.7 s. A small droplet of the good dispersed sample was placed separately on copper grids, which was precovered by a thin carbon film. A photographic plate of the TEM "JEOL JEM-1230" equipped with a CCD camera was used to detect the morphology and size of NC_{10} and NC_{12} operated at 120 kV.

Surface Tension Measurements

The surface tension of the synthesized quaternary surfactants was measured using a K6 tensiometer (Krüss, Germany) equipped with a Platinum-Iridium DuNouy ring at different temperatures (35, 45, and 55 °C). Distilled water with a surface tension of 70 $mN m^{-1}$ at 35 °C was used to prepare all concentrations (2.5×10^{-2} to 0.25 $mmol L^{-1}$). The ring was cleaned carefully using distilled water and acetone between the measurements.

Table 1 Observed elemental analysis and atomic absorption spectroscopy (AAS) for C₁₀ and C₁₂

Compounds	%C		%H		%N		%Fe	
	Calc.	Obs.	Calc.	Obs.	Calc.	Obs.	Calc.	Obs.
C ₁₀	33.70	33.41	6.74	6.42	3.93	3.89	15.73	15.63
C ₁₂	37.50	37.21	7.29	7.11	3.64	3.57	14.58	14.41

Antimicrobial Activities

The antimicrobial activities of C₁₀, C₁₂, NC₁₀, and NC₁₂ were evaluated at the Biotechnology Laboratory of Egyptian Petroleum Research Institute using the diffusion disc method against different bacteria, fungi, and yeast. *E. coli* and *P. aeruginosa* were tested as Gram-negative bacteria, *B. pumilus*, *M. luteus*, and *S. lutea* as Gram-positive bacteria, while the fungicidal activity was evaluated against *P. chrysogenum* as Filamentous Fungus and Yeast (*C. albicans*). The bacterial species grow on nutrient agar, fungi mold grows on Czapek's dox agar while the yeast grows on Wickerham medium. For Bacteria: The nutrient agar medium consists of 3 g L⁻¹ of beef extract, peptone (5 g L⁻¹), NaCl, and 20 g L⁻¹ agar, and the volume of the medium was then made to one liter using bidistilled water. The mixture was heated until boiling, and the media were sterilized by autoclave. For fungi: The dox agar medium consists of 30 g L⁻¹ sucrose, sodium nitrate (3 g L⁻¹), 0.5 g L⁻¹ of MgSO₄, KCl (0.5 g L⁻¹), FeSO₄ (0.01 g L⁻¹), dipotassium hydrogen orthophosphate (1 g L⁻¹), and 20 g L⁻¹ agar was then made to a volume to 1 L. The mixture was boiled and sterilized as mention before. For yeast, the medium consists of an equal weight of a yeast extract and malt extract (3 g L⁻¹), 10 g L⁻¹ of glucose and peptone (5 g L⁻¹). The nutrient agar, Dox media, and yeast media

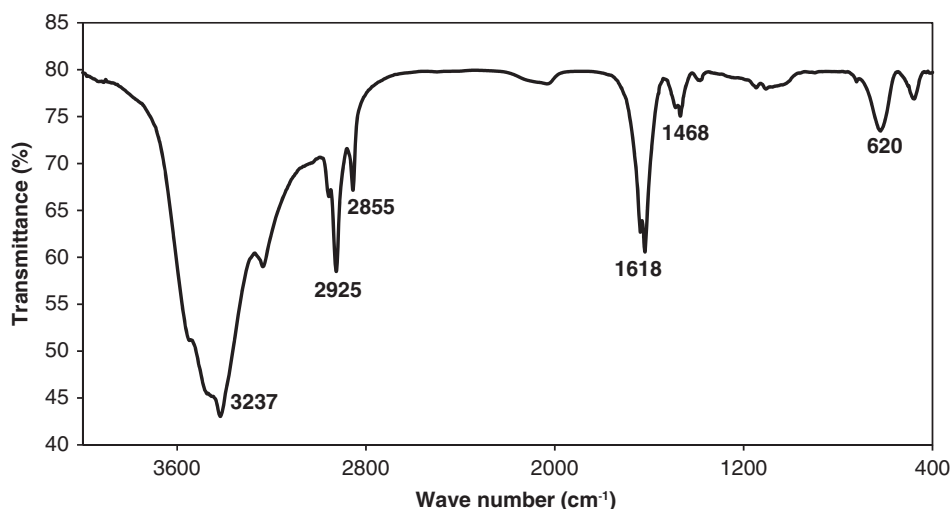
were inoculated with different microorganisms and incubated at 30 °C for 24 and 48 h in the case of bacteria and the yeast, respectively, while fungi were incubated at 28 °C for 48 h (Fox et al., 1990).

Results and Discussion

Characterization

The theoretical and experimental percentage of C, H, and N for C₁₀ and C₁₂ is listed in Table 1. The iron percentage of the prepared molecules obtained from atomic absorption spectroscopy measurements. The data revealed that the observed results are strongly agreeing with the calculated ones.

Figures 1 and S1 show the absorption bands of 2925 & 2855 cm⁻¹ and 2926 & 2855 cm⁻¹ caused by C-H_{st.} of C₁₀ and C₁₂, respectively. The peak appearing at 1468 cm⁻¹ is attributed to C-H_{def.} Also, the peak appearing at 3237 cm⁻¹ is attributed to the ammonium ion in RN⁺H₃. Peaks appearing at 1618 and 1619 cm⁻¹ are attributed to N-H bend of C₁₀ and C₁₂, respectively. Moreover, iron complexation bond appears at 620 and 623 cm⁻¹ of C₁₀ and C₁₂, respectively (Javidparvar et al., 2016).

**Fig. 1** FTIR spectrum of decylaminotetrachloroferrate (C₁₀)

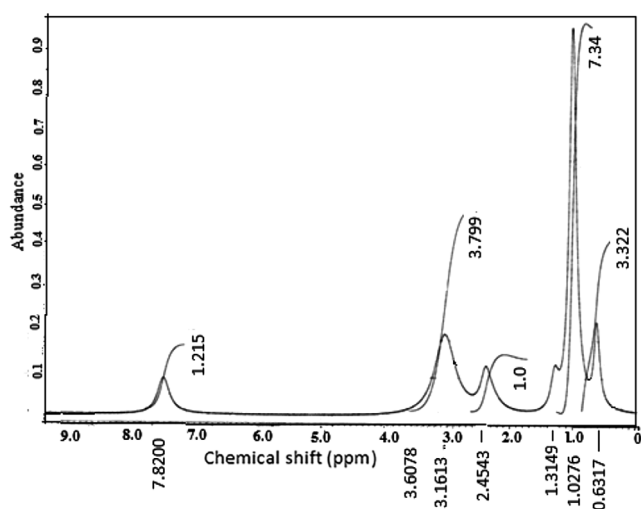


Fig. 2 ^1H -NMR spectrum of decylaminotetrachloroferrate (C_{10})

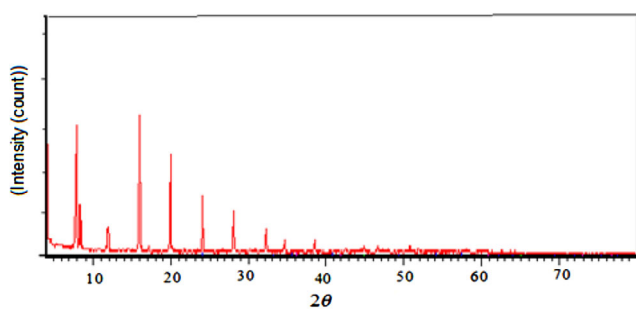


Fig. 3 XRD spectrum of decylaminotetrachloroferrate (C_{10})

^1H -NMR spectra of C_{12} (Fig. 2) and C_{10} compounds show $\delta = (0.6 \text{ \& } 0.63) \text{ ppm}$ for the $[\text{CH}_3]$ group, then $\delta = (1.00 \text{ \& } 1.02) \text{ ppm}$ for $[(\text{CH}_2)_n]$ groups, $\delta = (1.29 \text{ \& } 1.31) \text{ ppm}$ for

the $[\text{CH}_2-(\text{CH}_2)_n]$ group, $\delta = (2.48 \text{ \& } 2.46) \text{ ppm}$ for the $[\text{CH}_2\text{CH}_2-\text{N}^+]$ group, $\delta = (3.42 \text{ \& } 3.69) \text{ ppm}$ for the $[\text{N}^+-\text{CH}_2]$ group, and $\delta = 7.82 \text{ ppm}$ for the $[\text{N}^+\text{H}_3]$ group.

Figure 3 shows the XRD patterns of C_{10} , the diffractogram exhibits different distinct diffraction peaks at 2θ values of 8.4° , 15.9° , 20° , 24° , 28.1° , and 34.6° confirming the presence of iron in the prepared surfactants and are matched to other tetrachloroferrate derivatives in other work (Khazaei et al., 2018). XRD patterns of C_{12} have the nearest diffraction peaks and are present in Fig. S2.

Figure 4a, b shows the TEM micrograph of NC_{10} and NC_{12} , respectively. In Fig. 4a, the particle size ranged between 7.92 and 19.22 nm for NC_{10} , while in Fig. 4b, the size ranged between 16.63 and 18.84 nm for NC_{12} . The agglomeration of the prepared nanoparticles (Fig. 4) is due to van der Waals force and the high surface energy caused by the presence of iron. Moreover, in solution nanoparticles tend to minimize its interface by agglomeration. (Kocjan et al., 2017; Alia et al., 2016).

Critical Micelle Concentration

Critical micelle concentration (CMC) is defined as the concentration above which surfactant molecules tend to aggregate and form micelles. The variation in surface tension (γ) of the prepared molecules (C_{10} and C_{12}) is plotted versus log concentration as shown in Fig. 5 and the values of CMC at 35, 45, and 55 $^\circ\text{C}$ are listed in Table 2. It is obvious that, for the two prepared surfactants, the CMC values decreased by increasing the hydrophobic chain length (Shapovalov and Ponomariov, 2019; Shrestha and Yan, 2014). This indicates an increase in the

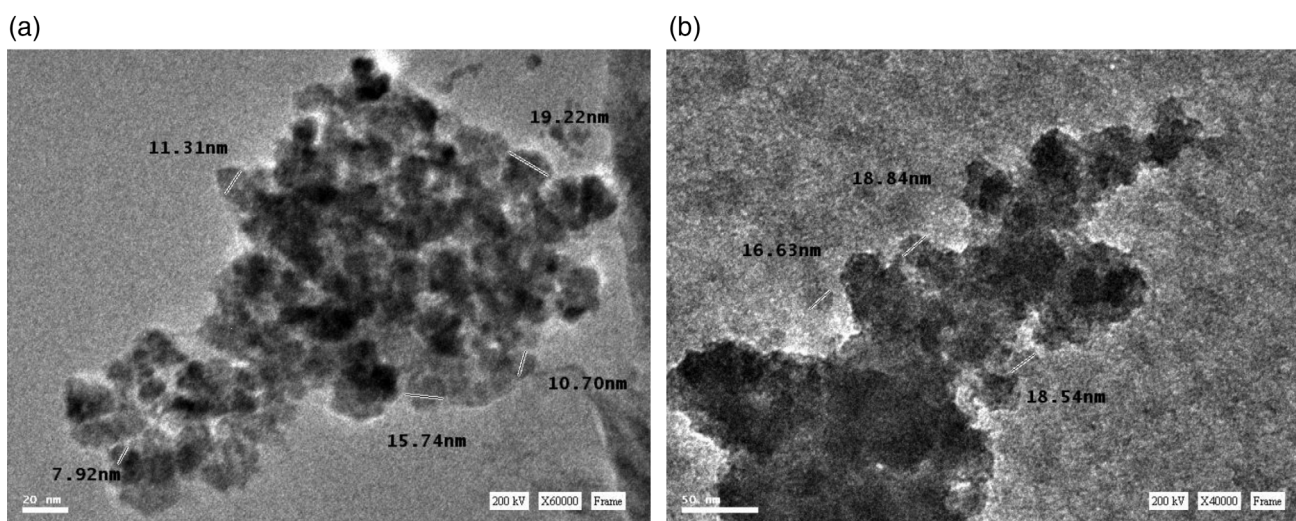


Fig. 4 TEM images of (a) C_{10} and (b) C_{12}

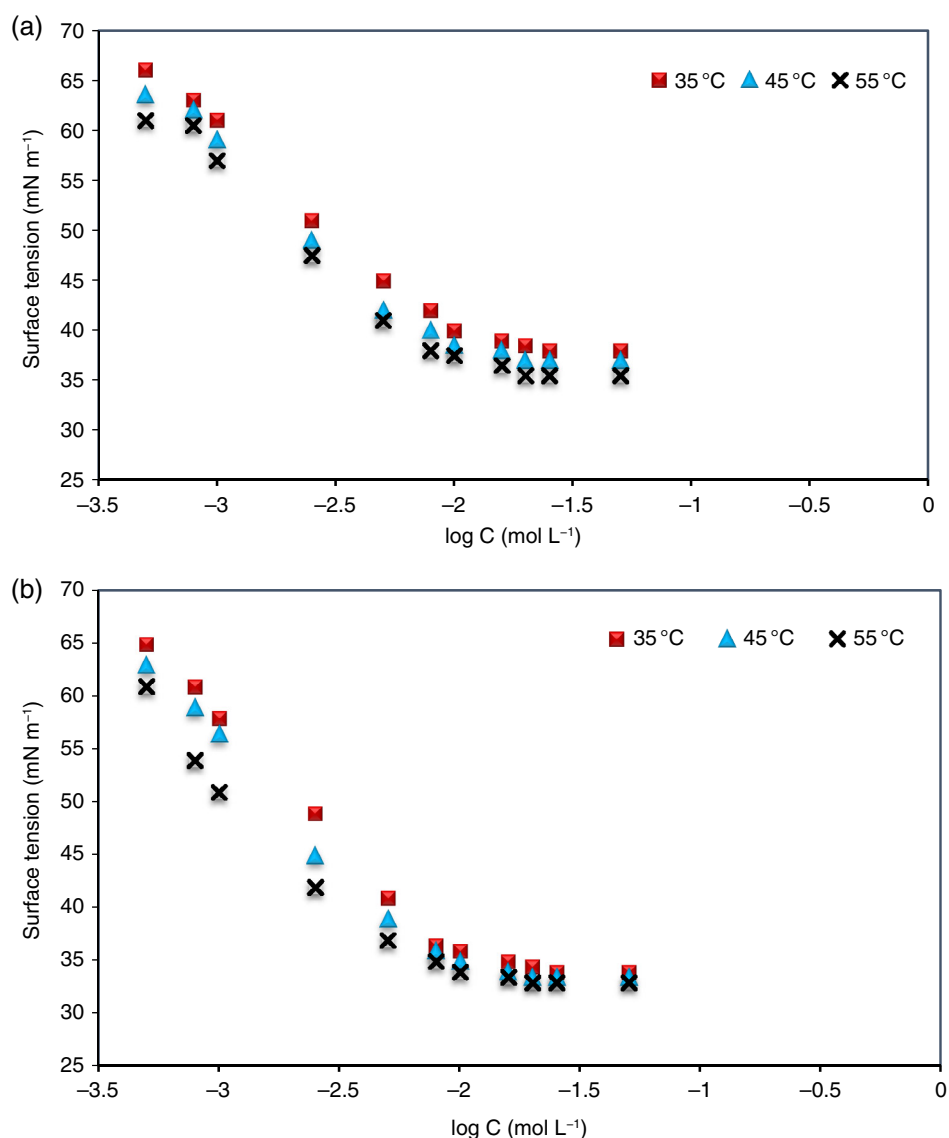


Fig. 5 The surface tension versus log C: (a) C₁₀ and (b) C₁₂

hydrophobicity of the surfactant molecules, which results in an increase in the repulsion between the hydrophobic chain and water molecules so that the surfactants tend to aggregate at a lower concentration (El Feky et al., 2016; Sun et al., 2013).

Also, the CMC values decrease upon increasing the temperature. This behavior of temperature increase causes a decrease in hydration of the hydrophilic group, which favors micellization. It seems from the data in Table 2 that an increase from C₁₀ to C₁₂ in the hydrophobicity made the surfactant more surface active.

Effectiveness (π_{CMC})

The effectiveness of a surfactant solution defined as the difference between the surface tension at the critical micelle

concentration (γ_{CMC}) and that of pure water (γ_0) at a given temperature (Hafiz et al., 2010). There is no much variation in the surface tension with the surfactant concentration above the CMC.

$$\pi_{\text{cmc}} = \gamma_0 - \gamma_{\text{cmc}} \quad (3)$$

The values of effectiveness corresponding to the prepared surfactants are calculated using Eq. (3) (Rosen and Kunjappu, 2012) and are listed in Table 2. The effectiveness values looked to be an agreeable variable comparing two surfactants in the same series. The more effective surfactant is that which gives a better reduction of the surface tension at its CMC. Concerning the values of π_{cmc} in Table 2, it observed that C₁₂ accomplished a higher π_{cmc} value. These differences in effectiveness in the prepared compounds were attributed to the difference in their

Table 2 Surface parameters of the investigated surfactants at different temperatures

Surfactant	Temp. (°C)	CMC × 10 ² (mol L ⁻¹)	π _{CMC} (mN m ⁻¹)	Γ _{max} × 10 ¹⁰ (mol cm ⁻²)	A _{min} (nm ²)
C ₁₀	35	0.89	30.00	4.12	0.40
	45	0.79	29.50	4.22	0.39
	55	0.72	29.00	4.04	0.41
C ₁₂	35	0.78	34.00	4.00	0.41
	45	0.74	33.50	4.63	0.36
	55	0.70	32.00	3.75	0.44

lipophilicity. Increasing the lipophilic chain length along C₁₀ and C₁₂ increases the effectiveness.

Maximum Surface Excess (Γ_{max}) and Minimum Surface Area (A_{min})

Γ_{max} is the number of surfactant molecules located in a unit area at the air/water interface. It calculated from the Gibbs equation (Rosen and Kunjappu, 2012):

$$\Gamma_{\max} = -\frac{1}{2.303nRT} \left(\frac{\partial \gamma}{\partial \log C} \right)_T \quad (4)$$

where Γ_{max} is the maximum surface excess concentration, R is the universal gas constant, and T is the absolute temperature. The values of Γ_{max} listed in Table 2 suggest that as the lipophilicity of the synthesized surfactant increases Γ_{max} values increase. This indicates that the surfactants are tightly packed at the A/W interface (Aydogan and Abbott, 2001).

From the results of Γ_{max} for the prepared surfactants listed in Table 2, it was concluded that increasing the alkyl chain from 10 to 12 carbon atoms leads to the adsorption of the surfactant at low concentrations, which shifts the Γ_{max} value to lower values. On the other hand, as the temperature increases from 35 to 45 °C, the number of surfactant molecules adsorbed at the interface increases, thus the Γ_{max} value increases.

Minimum surface area (A_{min}) is the average area occupied per adsorbed molecule at the interface given by (Rosen and Kunjappu, 2012):

$$A_{\min} = \frac{10^{14}}{N_A \Gamma_{\max}} \quad (5)$$

where N_A is the Avogadro's number and Γ_{max} (mol cm⁻²) is the maximum surface excess of adsorbed molecules at the interface. Decreasing Γ_{max} indicates a smaller number of the adsorbed surfactant molecules at the A/W interface. Hence, the area available for each molecule at the interface will increase, and this is an expected behavior. It is clear from Table 2 that increasing the hydrophobicity increases the value of A_{min}.

Thermodynamic Parameters

Thermodynamic parameters for micellization and adsorption of the synthesized surfactant molecules were calculated at 35, 45, and 55 °C using Gibbs' equations (Eqs. (6)–(11)) (Zdziennicka et al., 2012). For micellization,

$$\Delta G_{(\text{mic})}^{\circ} = RT \ln CMC \quad (6)$$

$$-\Delta S_{(\text{mic})}^{\circ} = d \left(\frac{\Delta G_{(\text{mic})}^{\circ}}{\Delta T} \right) \quad (7)$$

$$\Delta H_{(\text{mic})}^{\circ} = \Delta G_{(\text{mic})}^{\circ} + T \Delta S_{(\text{mic})}^{\circ} \quad (8)$$

For adsorption,

$$\Delta G_{(\text{ads})}^{\circ} = \Delta G_{(\text{mic})}^{\circ} - 6.023 \times 10^{-1} \times \pi_{\text{CMC}} \times A_{\min} \quad (9)$$

$$-\Delta S_{(\text{ads})}^{\circ} = d \left(\frac{\Delta G_{(\text{ads})}^{\circ}}{\Delta T} \right) \quad (10)$$

$$\Delta H_{(\text{ads})}^{\circ} = \Delta G_{(\text{ads})}^{\circ} + T \Delta S_{(\text{ads})}^{\circ} \quad (11)$$

The standard free energies of micellization (ΔG_(mic)[∘]) and adsorption (ΔG_(ads)[∘]) are negative indicating spontaneous processes (El-Shamy and Nessim, 2017). The prepared surfactants have a higher tendency to adsorb at the interface than forming micelles (ΔG_(ads)[∘] > ΔG_(mic)[∘]). Also, it was noticed that ΔG_(mic)[∘] becomes more negative as the temperature increases, hence favoring micellization. The standard entropy changes of micellization (ΔS_(mic)[∘]) showed decrease than those of adsorption (ΔS_(ads)[∘]) for the prepared surfactants (Table 3), indicating the lower ordering of the adsorbed molecules rather than molecules in the micellization state. This is attributed to the compacting of the hydrophobic chain within the micelles, which leads to a great extent of ordering of the molecules (Desai and Banat, 1997). Positive values of ΔH_(mic)[∘] indicate the endothermic micellization process. The change of the standard heat

Table 3 Thermodynamic parameters of micellization and adsorption of the investigated surfactants at different temperatures

Surfactant	Temp. (°C)	ΔG° (kJ mol ⁻¹)		ΔS° (kJ (mol K) ⁻¹)		ΔH° (kJ mol ⁻¹)	
		Mic.	Ads.	Mic.	Ads.	Mic.	Ads.
C ₁₀	35	-12.09	-12.10	—	—	8.85	9.46
	45	-13.00	-13.01	0.068	0.070	8.62	9.25
	55	-13.45	-13.46	—	—	8.85	9.50
C ₁₂	35	-12.43	-12.43	—	—	4.78	4.50
	45	-12.98	-12.98	0.056	0.055	4.84	4.51
	55	-13.53	-13.54	—	—	4.83	4.50

enthalpy of micellization $\Delta H_{(\text{mic})}^\circ$ is inversely proportional to the alkyl chain.

Antimicrobial Activity of the Synthesized Quaternary Surfactants

The data listed in Table 4 show that C₁₀, C₁₂, NC₁₀, and NC₁₂ have a significant antimicrobial activity toward all the tested organisms. The inhibition zone diameter of the tested species increases as the hydrophobicity increases from C₁₀ to C₁₂. The external surface of the bacteria carries a net negative charge that is neutralized by divalent cations Mg(II) and Ca(II) (Gilbert and Moore, 2005; Shaban et al., 2014). This links with the teichoic acid and polysaccharide parts of Gram-positive bacteria and the lipopolysaccharide of Gram-negative bacteria, and the cytoplasmic membrane itself. According to the last description, cationic antimicrobial agents possess high ability to join the cell membrane of bacteria (Aiad et al., 2016; Walsh and Amyes, 2004). The studied surfactants (C₁₀, C₁₂, NC₁₀, and NC₁₂) carried net positive charge on the nitrogen atom with different hydrophobic chain lengths (normal alkyl chains) in order to study the hydrophobic effect on the interaction with the cell membrane. The cationic surfactants interacted with the cell wall substituting for the divalent cations.

From a thermodynamic aspect, C₁₂ has a higher tendency for adsorption than C₁₀. Moreover, C₁₂ has a higher negative value of free energy of micellization that facilitates the solubilization of the bacterial cell (hydrophobic components) on the micelle core.

The data listed in Table 4 showed that the antibacterial activities of nanopowder forms (NC₁₀ and NC₁₂) are higher than their parent surfactants. This may be attributed to their small particle size, which facilitates permeability of these nanomolecules through the cell membrane. Intermediate size between the parent C₁₂ and NC₁₂ was obtained for dodecylamino tetrachloroferrate and abbreviated as MC₁₂, which was obtained after ball milling of 4 h (200 rpm) to evaluate the effect of particle size on its antimicrobial activity using the same agar diffusion technique. The results listed in Table 5 show that in the case of yeast, MC₁₂ has the most inhibition efficiency. While, in the case of Gram-negative bacteria, this intermediate size (MC₁₂) gives intermediate results between parent and nanoparticles. So, small particle size is recommended. In the case of Gram-positive bacteria, the inhibition efficiency of MC₁₂ decreases linearly with the particle size (Table 4). In addition, after using different Gram-positive species (Table 5), the inhibition efficiency of dodecylamino tetrachloroferrate on Gram-negative species is higher than that of positive species. This may be explained by the difference in the cell wall width

Table 4 Antimicrobial activity of the synthesized surfactants and their nanopowders against different pathogenic bacteria and fungi

Compounds	Inhibition zone diameter (mm)						
	Gram-positive			Gram-negative		Yeast	Fungi
	<i>Bacillus pumilus</i>	<i>Micrococcus luteus</i>	<i>Sarcinalutea</i>	<i>Pseudomonas aeruginosa</i>	<i>Escherichia coli</i>	<i>Candida albicans</i>	<i>Penicilliumchrysogenum</i>
Erythromycin	32	32	44	30	32	—	—
Metronidazole	—	—	—	—	—	27	25
C ₁₀	21	32	36	24	33	25	28
C ₁₂	28	45	34	22	37	37	31
NC ₁₀	26	41	33	23	51	50	33
NC ₁₂	21	40	36	26	31	35	32

Table 5 Antimicrobial activity of MC₁₂ against different pathogenic bacteria and fungi

Compounds	Inhibition zone diameter (mm)					
	Gram-positive		Gram-negative		Yeast	Fungi
	<i>Bacillus subtilis</i>	<i>Staphylococcus aureus</i>	<i>Pseudomonas aeruginosa</i>	<i>Escherichia coli</i>	<i>Candida albicans</i>	<i>Aspergillus niger</i>
Erythromycin	29	28	28	30	—	—
Metronidazole	—	—	—	—	27	30
MC ₁₂	35	36	25	26	39	41

between Gram-negative (3–4 nm) and Gram-positive bacteria (30 nm), which were composed of peptidoglycan. (Chatterjee et al., 2015)

Conclusions

Two cationic surfactants were prepared and characterized using different techniques. The surface activity of the two prepared surfactants increases with the hydrophobicity. Thermodynamic parameters of adsorption and micellization were calculated. The free energy of micellization and adsorption indicate that C₁₂ has a higher tendency for micellization and adsorption rather than C₁₀. The powder form of the two surfactants was obtained using the ball mill technique. The biological activity of the prepared surfactants was investigated in addition to their nanosize. C₁₂ has good microbial activity compared with C₁₀, while NC₁₀ showed very excellent biological activity against fungi, yeast, Gram-negative, and Gram-positive bacteria. These results indicate that small particle size of NC₁₀ facilitates the permeability of the nanopowders through the cell membranes.

Conflict of Interest The authors declare that they have no conflict of interest.

References

- Aiad, I., Riya, M. A., Tawfik, S. M., & Abosehly, M. A. (2016) Synthesis, surface properties and biological activity of *N,N,N*-tris (hydroxymethyl)-2-oxo-2-chloride surfactants. *Egyptian Journal of Petroleum*, **25**:299–307. <https://doi.org/10.1016/j.ejpe.2015.07.020>
- Ali, A., Zafar, H., Zia, M., ul Haq, I., Phull, A. R., Ali, J. S., & Hussain, A. (2016). Synthesis, characterization, applications, and challenges of iron oxide nanoparticles. *Nanotechnology, Science and Applications*, **9**:49–67.
- Aydogan, N., & Abbott, N. L. (2001) Interfacial properties of unsymmetrical bolaform amphiphiles with one ionic and one nonionic head group. *Journal of Colloid and Interface Science*, **242**: 411–418.
- Berti, D., & Palazzo, G. (2014) *Colloidal foundations of nanoscience*. Netherlands: Elsevier.
- Chanawanno, K., Chantapromma, S., Anantapong, T., Kanjana-Opas, A., & Fun, H.-K. (2010) Synthesis, structure and in vitro antibacterial activities of new hybrid disinfectants quaternary ammonium compounds: Pyridinium and quinolinium stilbene benzenesulfonates. *European Journal of Medicinal Chemistry*, **45**: 4199–4208.
- Chatterjee, T., Chatterjee, B. K., Majumdar, D., & Chakrabarti, P. (2015) Antibacterial effect of silver nanoparticles and the modeling of bacterial growth kinetics using a modified Gompertz model. *Biochimica et Biophysica Acta (BBA)-General Subjects*, **1850**: 299–306.
- Desai, J. D., & Banat, I. M. (1997) Microbial production of surfactants and their commercial potential. *Microbiology and Molecular Biology Reviews*, **61**:47–64.
- Dunkley, R. W. S. (2004) Nanotechnology: social consequences and future implications. *Futures*, **10**:1129–1132.
- Eastoe, J., & Tabor, R. F. (2014) Surfactants and nanoscience. In D. Berti, G. Palazzo, (Ed.), *Colloidal foundations of nanoscience* (pp. 135–157). Netherlands: Elsevier.
- El Feky, A. A., Shalaby, M. N., El-Shamy, O. A. A., & Selim, S. A. (2010) Adsorption of some surfactants onto polyvinyl alcohol as hydrophobic polymer surface. *Journal of Dispersion Science and Technology*, **31**:1091–1099.
- El Feky, A. A., Shalaby, M. N., El-shamy, O. A. A., & Suzy, A. (2016) Surface activity and adsorption of some surfactants at aqueous / air interface at different temperatures. *International Journal of Scientific & Technology Research*, **5**:179–184.
- El-Fawal, E. M., & El-Shamy, O. A. A. (2019) Photodegradation enhancement of 2-chlorophenol using ZnO–CdS@CS nanocomposite under visible light. *International Journal of Environmental Science and Technology*. <https://doi.org/10.1007/s13762-019-02249-y>
- El-Shamy, O. A. A., & Nessim, M. I. (2017) Surface activities and quantum chemical calculations for different synthesized cationic gemini surfactants. *Tenside Surfactants Detergents*, **54**:443–447.
- Fox, A., Morgan, S. L., Larsson, L., & Odham, G. (1990) *Analytical microbiology methods*. New York, NY: Springer.
- Fraise, A. P., Lambert, P. A., & Maillard, J.-Y. (2008) *Russell, Hugo & Ayliffe's principles and practice of disinfection, preservation & sterilization*. Hoboken, NJ: John Wiley & Sons.
- Garcia, M. T., Campos, E., Sanchez-Leal, J., & Ribosa, I. (2000) Anaerobic degradation and toxicity of commercial cationic surfactants in anaerobic screening tests. *Chemosphere*, **41**:705–710.
- Gaze, W. H., Abdoulsalam, N., Hawkey, P. M., & Wellington, E. M. H. (2005) Incidence of class 1 integrons in a quaternary ammonium compound-polluted environment. *Antimicrobial Agents and Chemotherapy*, **49**:1802–1807.
- Gilbert, P., & Moore, L. E. (2005) Cationic antiseptics: diversity of action under a common epithet. *Journal of Applied Microbiology*, **99**:703–715.
- Hafiz, A. A., Badawi, A. M., El-Deeb, F. I., Soliman, E. A., El-Awady, M. Y., & Mohamed, D. E. (2010) Ferrocene-based cationic

- surfactants: Surface and antimicrobial properties. *Journal of Surfactants and Detergents*, **13**:165–172.
- Ishikawa, S., Matsumura, Y., Yoshizako, F., & Tsuchido, T. (2002) Characterization of a cationic surfactant-resistant mutant isolated spontaneously from *Escherichia coli*. *Journal of Applied Microbiology*, **92**:261–268.
- Javidparvar, A. A., Ramezanzadeh, B., & Ghasemi, E. (2016) The effect of surface morphology and treatment of Fe₃O₄ nanoparticles on the corrosion resistance of epoxy coating. *Journal of the Taiwan Institute of Chemical Engineers*, **000**:1–11. <https://doi.org/10.1016/j.jtice.2016.01.001>
- Khazaei, A., Moosavi-Zare, A. R., Firoozmand, S., & Khodadadian, M. R. (2018) Synthesis, characterization and application of 3-methyl-1-sulfonic acid imidazolium tetrachloroferrate as nanostructured catalyst for the tandem reaction of β -naphthol with aromatic aldehydes and amide derivatives. *Applied Organometallic Chemistry*, **32**:e4058.
- Khidr, T. T., Doheim, M. M., & El-Shamy, O. A. A. (2015) Effect of ethoxylate on pour point depressant of fuel oil. *Energy Sources, Part A: Recovery, Utilization, and Environmental Effects*, **37**:1697–1703.
- Kocjan, A., Logar, M., & Shen, Z. (2017) The agglomeration, coalescence and sliding of nanoparticles, leading to the rapid sintering of zirconia nanoceramics. *Scientific Reports*, **7**:1–8. <https://doi.org/10.1038/s41598-017-02760-7>
- Kourai, H., Yabuhara, T., Shirai, A., Maeda, T., & Nagamune, H. (2006) Syntheses and antimicrobial activities of a series of new bis-quaternary ammonium compounds. *European Journal of Medicinal Chemistry*, **41**:437–444.
- Rosen, M. J., & Kunjappu, J. T. (2012) *Surfactants and interfacial phenomena*. Hoboken, NJ: John Wiley & Sons.
- Shaban, S. M., Aiad, I., El-Sukkary, M. M., Soliman, E. A., & El-Awady, M. Y. (2014) Synthesis, surface, thermodynamic properties and biological activity of dimethylaminopropylamine surfactants. *Journal of Industrial and Engineering Chemistry*, **20**:4194–4201.
- Shapovalov, S., & Ponomariov, V. (2019) Interaction of dyes with cationic surfactants in solutions: Determination of critical micelle concentration. *International Letters of Chemistry, Physics and Astronomy*, **81**:27–34. <https://doi.org/10.18052/www.scipress.com/ILCPA.81.27>
- Shrestha, Y. K., & Yan, F. (2014) Determination of critical micelle concentration of cationic surfactants by surface-enhanced Raman scattering. *RSC advances*, **4**:37274–37277. <https://doi.org/10.1039/c4ra05516k>
- Sun, Y.-Q., Li, W.-J., Wang, W.-X., Li, Q.-X., Hreczuch, W., & Sulek, W. (2013) Synthesis and performance of polyoxy-ethylene ester quaternary ammonium salt. *Tenside Surfactants Detergents*, **50**:9–13.
- Tezel, U. (2009) Fate and effect of quaternary ammonium compounds in biological systems. Georgia Institute of Technology, Atlanta.
- Walsh, F. M., & Amyes, S. G. B. (2004) Microbiology and drug resistance mechanisms of fully resistant pathogens. *Current Opinion in Microbiology*, **7**:439–444.
- Zdziennicka, A., Szymczyk, K., Krawczyk, J., & Jańczuk, B. (2012) Critical micelle concentration of some surfactants and thermodynamic parameters of their micellization. *Fluid Phase Equilibria*, **322**:126–134.